NDT&E International 164 (2026) 103807

Contents lists available at ScienceDirect

NDT and E International

journal homepage: www.elsevier.com/locate/ndteint

Monitoring the viscoelastic evolution of vinyl ester resins for SMC via non-contact resonant ultrasound spectroscopy

Lola Fariñas [a,b,*,1], Beatriz Achiaga [c], Marta Camacho-Iglesias [d], Rafael García-Etxabe [d]

[a] DeustoTech, Faculty of Engineering, University of Deusto, Bilbao, Spain
[b] Ikerbasque, Basque Foundation for Science, Bilbao, Spain
[c] Mechanics, Design and Industrial Engineering Department, Faculty of Engineering, University of Deusto, Bilbao, Spain
[d] GAIKER, Technology Centre, Basque Research and Technology Alliance, Zamudio, Spain

ARTICLE INFO

Keywords:
Air-Coupled Ultrasound (ACU)
Non-Contact Resonant Ultrasound Spectroscopy (NC-RUS)
Sheet Moulding Compound (SMC)
Resin maturation
Viscoelasticity
Polymer monitoring

ABSTRACT

Monitoring the pre-cure maturation of thermosetting resins, particularly in Sheet Moulding Compound (SMC) manufacturing, is critical for ensuring processability and final part quality. This stage involves complex viscoelastic changes driven by ionic thickening, a process often classified using industrial know-how rather than robust quantitative methods. However, current standard characterization methods remain destructive or contact-based, hindering their use for continuous, in-situ monitoring. This study presents a contactless methodology based on Non-Contact Resonant Ultrasound Spectroscopy (NC-RUS), implemented via Air-Coupled Ultrasound (ACU) to monitor the maturation of vinyl ester (VE) resin over a 30-day period. We compared a neat resin control against a formulation thickened with 3 wt% magnesium oxide (MgO). Ultrasonic parameters, estimated from thickness resonance spectra, show that, for the thickened samples, both longitudinal velocity and attenuation increase significantly with time, in contrast to the control samples confirming the ultrasonic sensitivity to the ionic thickening of the VE. Furthermore, the trends in longitudinal modulus and attenuation were validated against a standard curve of apparent viscosity obtained via Brookfield viscometry. This points to a correlation with the phenomenological stages of SMC maturation. These findings show the potential of ACU as a powerful contactless tool for the in-situ monitoring of resin pre-cure state in composite manufacturing.

1. Introduction

Vinyl ester resins are a critical class of thermosetting polymers widely used in the manufacture of high-performance composite materials due to their excellent mechanical properties, corrosion resistance, and thermal stability, as well as their lower cost compared to other popular thermosets, such as epoxies [1,2]. A significant industrial application for these resins is in Sheet Moulding Compound (SMC), a composite prepreg used extensively in the automotive, aerospace, electrical, and construction sectors to manufacture complex, lightweight, and durable parts and enclosures. The SMC manufacturing process involves a crucial, yet challenging, maturation or thickening stage prior to curing, wherein the initial low-viscosity resin paste is transformed into a handleable sheet suitable for compression moulding [3].

The controlled evolution of viscosity during this maturation phase is paramount for ensuring final part quality, process efficiency and cost savings [4]. This step is highly sensitive to extrinsic factors, including batch-to-batch variations in raw materials, ambient temperature, and humidity, making its precise control a persistent challenge in industrial settings [5].

Despite its importance, the *in-situ* chemorheological monitoring of SMC maturation is hindered by the limitations of conventional methods, which fail to capture the transient, physical nature of the process. The thickening is governed by the formation of ionic networks, not permanent covalent chain extension, a distinction that invalidates some standard analytical correlations. For instance, correlating bulk rheology with molecular weight via Gel Permeation Chromatography (GPC) is fundamentally flawed, as the sample dissolution required for analysis destroys the ionic associations [6,7]. Similarly, while FTIR spectroscopy can confirm the initial acid-base reaction, it is insensitive to the formation of the physical ionic clusters that dominate the viscoelastic

* Corresponding author. DeustoTech, Faculty of Engineering, University of Deusto, Bilbao, Spain.
E-mail address: lola.farinas@csic.es (L. Fariñas).
[1] Present address: Institute for Physical and Information Technologies (ITEFI), Spanish National Research Council (CSIC), Serrano 144, Madrid, 28006, Spain.

https://doi.org/10.1016/j.ndteint.2026.103807
Received 18 March 2026; Received in revised form 29 June 2026; Accepted 29 June 2026
Available online 29 June 2026

response [8]. This analytical gap highlights the critical need for a technique capable of tracking the evolution of the material's physical state. While offline rheological analysis provides direct measurement of viscosity, it is inherently destructive, requires sample extraction, and cannot offer the continuous, in-situ data required for modern process analytical technology and Industry 4.0 paradigms [9,10].

Therefore, a critical need is established for a non-destructive, non-invasive technique capable of monitoring the evolution of the resin state throughout the maturation period. Ultrasonic waves have long been used as a non-destructive tool for characterizing polymer dynamics, as wave propagation parameters are intrinsically linked to the complex mechanical moduli of the medium [11–14]. The foundational work of Rokhlin et al. [15] demonstrated that both velocity and attenuation are highly sensitive to the kinetics of network formation in epoxy resins, enabling a real-time tracking of the transition from the viscous liquid to the solid state. Building on this, Challis and co-authors made significant contributions to the quantitative characterization of viscoelastic polymer networks: Freemantle and Challis [16] measured simultaneously both shear and compression wave parameters in curing adhesives, while Challis et al. [17] established ultrasound as a reliable method for following network formation in epoxy systems, validating it against dielectric and nuclear magnetic resonance data. These approaches have been extended and applied across a wide range of thermosetting systems and frequency regimes, confirming the ongoing relevance of ultrasonic monitoring for polymer characterization [18–22]. According to the comprehensive review by Lakes [23], resonance-based methods and wave propagation techniques bridge the gap between molecular-scale interactions and bulk rheological behavior across a broad frequency range, a principle underpinning the present study.

Ideally, viscoelastic changes would be monitored through the excitation of shear waves, which directly couple to shear modulus (G) and viscosity [24]. However, G is close to zero in liquid and semi-solid media, making shear wave excitation often unfeasible in the early stages of resin maturation [25,26]. Furthermore, the high attenuation characteristics of evolving polymers frequently require complex guided wave setups or contact-based transducers to achieve sufficient signal-to-noise ratios, as demonstrated by Simonetti and Cawley [27] for highly attenuative viscoelastic materials. To overcome this limitation, non-contact ultrasonic methods have been explored for monitoring the curing of thin epoxy adhesives and polyester resins: Dixon et al. [28] demonstrated the non-contact measurement of shear and compression moduli in curing epoxy adhesives, while Lionetto et al. [29] applied air-coupled ultrasound to cure monitoring of polyester resins. For the particular case of the resin maturation stage, where unlike curing, no permanent chemical bonds are formed but rather a reversible ionic physical network, this work proposes the use of Non-Contact Resonant Ultrasound Spectroscopy (NC-RUS) via Air-Coupled Ultrasound (ACU) technology to monitor longitudinal wave parameters as indicators of its viscoelastic evolution. Based on previous works studying the evolution of shear and longitudinal parameters during curing [29,30], we hypothesize that the formation of the ionic network, while predominantly a shear phenomenon, induces measurable changes in both longitudinal attenuation and velocity that can serve as a proxy for resin state determination.

In this context, the specific objectives of this study are threefold: (i) to contactlessly monitor the long-term evolution of longitudinal ultrasonic velocity and attenuation in vinyl ester resins prior to curing; (ii) to evaluate the method by verifying the stability comparing a thickened formulation against a neat control group, ensuring that observed changes are exclusively driven by the thickening mechanisms; and (iii) to validate these ultrasonic parameters by relating them with the maturation stages estimated based on standard Brookfield viscometry.

2. Theoretical background

2.1. Viscoelasticity in pre-curing resins

One of the main steps in the manufacture of SMC prepregs based on vinyl ester formulations is the evolution of the system's viscosity from a liquid state to a semisolid non-tacky sheet. This key step is the thickening, which is achieved not through premature radical polymerization, but via a controlled acid-base reaction between residual carboxylic acid groups on the polymer backbone and a metallic oxide, most commonly magnesium oxide (MgO). This reaction does not form permanent covalent bonds but rather establishes a physical network based on coordinate ionic complexes. As these ionic domains grow and associate, they restrict the long-range mobility of the polymer chains. Macroscopically, this manifests as a dramatic increase in viscosity and the transition from a Newtonian fluid to a viscoelastic semi-solid [31,32].

2.2. Ultrasonic wave propagation in viscoelastic media

The ultrasonic wave propagation through a viscoelastic medium is governed by the longitudinal modulus (M), which accounts for the material resistance to deformation under a longitudinal wave. M is related to the bulk modulus (K) and shear modulus (G) by Ref. [25]:

$$M = K + \frac{4}{3}G \tag{1}$$

In the context of resin maturation, the thickening process is driven by the increase in the resistance to flow (viscosity) and the formation of a preliminary physical network which predominantly affects the G. Although for a liquid and semi-solid resin it is expected that K is typically orders of magnitude larger than G, implying that the longitudinal velocity (v_L) is dominated mainly by compressibility, the evolution of the resin from a liquid to a gel or semi-solid involves a drastic change in G too.

Consequently, while the real part of the longitudinal modulus is directly related to stiffness and density evolution ($M = p \cdot v_L^2$), the imaginary part is linked to energy dissipation. Hence, the ultrasonic attenuation (α) can be also linked with energy losses as a consequence of relaxation mechanisms of the polymer chains as they become restricted by ionic crosslinking. Thus, by monitoring both v_L and α, we can establish an indirect correlation with the rheological thickening usually measured by resistance to flow or viscosity.

3. Materials and methods

3.1. Resin formulation

The material studied was Derakane™ 760 from INEOS (London, UK), an epoxy vinyl ester (VE) resin widely employed in the SMC and related composite industry for high-performance applications. Two distinct formulations were prepared for comparison in order to isolate the thickening effect:

- VE-Ref: the control formulation, consisting of neat VE resin with 1.5 wt % of PEROXAN PO from PERGAN (Frankfurt, Germany) as peroxide initiator, the primary catalyst.
- VE-MgO: the thickened formulation, prepared by mixing the VE resin with 3.0 wt % LUVATOL MK-35 from LEHVOSS (Hamburg, Germany) and 1.5 wt % of PEROXAN PO.

The initiator was included in both formulations, although not expected to induce thermal cross-linking at the experimental temperature (23 ± 2 °C), its presence accounts for any passive contributions to the material's initial viscoelastic properties. The formulations and the resin samples were pre-conditioned and stored in a temperature-controlled laboratory for the duration of the study. Accordingly, all experimental

measurements (both Brookfield rotational viscometry and non-contact ultrasonic testing) were also performed at this temperature range in the lab to eliminate any temperature-induced rheological artifacts.

3.2. Sample containment

Due to the liquid state of the resin, a specific sample holder was required. The needed criteria that were (i) chemically inert, (ii) equipped with a lid to prevent volatile monomer loss, and (iii) be ultrasonically transparent at the working frequencies used or alternatively, have a response that can be easily decoupled from the frequency window of relevance for the samples under study. To satisfy these requirements, a commercial cylindrical aluminum holder (68 mm diameter) with a removable lid and a thin base (0.3 mm) was used for all experiments. The holder's diameter was selected to exceed that of the transducers' beam width to simplify alignment and prevent edge diffraction effects (Fig. 1).

3.3. Air-Coupled Ultrasonic (ACU) setup and data processing

The physical evolution of the resin in the pre-cure stages was monitored using a non-contact, through transmission ultrasonic technique based on the excitation and sensing of thickness resonances (Non-Contact Resonant Ultrasound Spectroscopy, NC-RUS). The governing principle is that when a plane wave is normally incident on a sample, constructive interference occurs at specific frequencies (f_n) where the sample thickness (d) is a multiple (n) of half the wavelength of the ultrasonic propagation velocity within the material (v_L). This condition give rise to a series of resonance peaks in the transmission spectrum, described by (2) [33]:

$$f_n = n\frac{v_L}{2d}\ (n = 1, 2, 3, \ldots) \tag{2}$$

By identifying these resonant frequencies in the experimentally measured spectrum, ultrasonic parameters can be directly estimated assuming an analytical expression for the transmission coefficient (γ) such as in (3) and an attenuation coefficient (α) that varies with the frequency following a power law (4):

$$\gamma = \frac{-2Z_oZ_s}{2Z_oZ_s\cos\left(\frac{2\pi f_0}{v_L}\right)d + i\left(Z_o^2 + Z_s^2\right)\sin\left(\frac{2\pi f_0}{v_L}\right)d} \tag{3}$$

$$\propto = \propto_0 \left(f/f_0\right)^n \tag{4}$$

where Z_o and Z_s are the acoustic impedance of the medium (air) and the sample.

The experimental setup consisted of a through-transmission configuration with ultrasonic transducers aligned for normal incidence (Fig. 1a). A pair of high-sensitivity, wideband air-coupled piezoelectric transducers (US-BioMat lab, CSIC, Spain) with a working frequency range of 135 - 350 kHz were used. The sample, held within the aluminum containment (see section 3.2), was placed in a holder between the transducers. During each ultrasonic acquisition, the lid was temporarily released (less than 1 min in total including placing the container in the holder, releasing the lid, and performing the average signal capture) (see Fig. 1b). The transmitter was excited by a spike pulse from a commercial pulser/receiver (DPR300, JSR, PA, USA), and the received signal was amplified with a gain set between 60 and 70 dB during sample monitoring. A digital oscilloscope (MSO44B, Tektronix, WA, USA), synchronized with the pulser, digitized the received signals at a sampling rate of 2.5 MS/s, averaging 32 consecutive acquisitions to enhance signal-to-noise ratio (SNR).

The acquired time-domain data were processed offline using Matlab (Mathworks, MA, USA) and Python (v. 3.9.13). Waveforms were converted to the frequency domain via Fast Fourier Transform (FFT). The transmission coefficient spectrum was then calculated by subtracting the blank calibration reference. Finally, ultrasonic parameters such as longitudinal velocity, attenuation, resonant frequency, or sample thickness were determined from the thickness resonance patterns measured in the spectra using equation (2). A more detailed description of the experimental procedure and analysis can be found in previous works [34–36].

To systematically evaluate the maturation process, two distinct sets of resin samples were monitored over an extended period: a neat control formulation (VE-Ref) and the chemically thickened resin (VE-MgO). Three independent replicates of the VE-Ref formulation were measured at strategic verification intervals (Days 0, 1, 3, 8 and 16) to confirm baseline stability, while the six independent replicates of the VE-MgO formulation were monitored daily for up to 30 days to capture thickening kinetics. All experimental results are presented as mean values accompanied by their respecting standard deviations. Statistical fitting and regression analyses were performed as specified in the respective results figures.

3.4. Brookfield viscometry

Standard rheological behavior of the VE-MgO, specifically its apparent viscosity, was obtained using a Brookfield viscometer (DVE EHB TJ0 mounted onto a D220 Helipath stand) designed to slowly lower or raise the system, so that its rotating T-bar spindle describes a helical

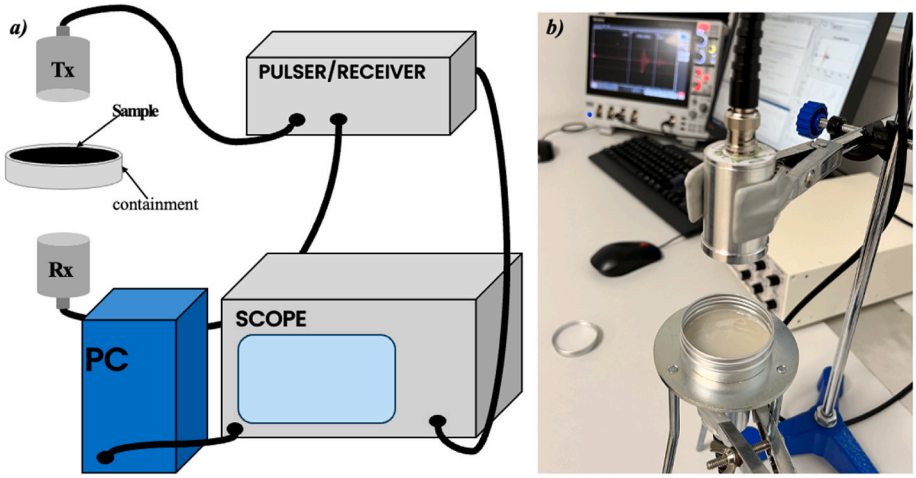

Fig. 1. Experimental ultrasonic setup: a) Schematic diagram of the whole ACU system; b) Picture showing the air-coupled transducers aligned for normal incidence through the sample and the containment.

path through the test sample. T-bar spindles (Helipath Spindle Set, Brookfield AMETEK, Massachusetts, USA) of different sizes were used to ensure stability of the measurement percentage across the different measurements.

Brookfield viscosity measurements were performed over the same 30-day maturation period at regular time intervals, with measurements taken on days 1, 2, 3, 4, 7, 9, 11, 14, 16, 18, 21, 23, 25, 28, 30. All viscosity tests were carried out at 23 ± 2 °C. The spindle size and the rotational speed were selected according to the consistency of the sample to maintain the torque reading within the recommended operating range. However, during the initial unreacted phase (days 0–1), the viscosity was too low to reach this target even under maximum speed conditions. As the thickening progressed, the settings were dynamically adjusted to maintain the spring torque as close to 50% as possible. The measurement conditions were reported in terms of spindle geometry, rotation speed, and temperature (see Table 1).

3.5. Other measurements

A Nahita Blue Series 5133 precision balance (FugelabGB10, Navarra, Spain) was employed in the formulation stage of every sample as well as tracking their weight change along the period studied.

4. Results

4.1. Viscosity and resin maturation stages

The rheological behavior of the VE-MgO formulation, measured via Brookfield viscometry over a 30-day period, is presented in Fig. 2. The viscosity curve serves as the reference standard for defining the maturation progress.

Five distinct phenomenological stages were identified based on the slope changes and absolute viscosity values, consistent with industrial SMC classifications [6,31,37]. Usually, this classification attends to qualitative indicators which are mostly based on hands-on experience as can be seen on the description on Table 2. However, correlations are expected with slope changes in the viscosity-time curve of the resin.

4.2. Physical changes during maturation

Fig. 3 summarizes the physical evolution of both the control (VE-Ref) and thickened (VE-MgO) samples. Regarding weight stability (Fig. 3a), both formulations exhibited a monotonic linear weight loss over the 30-day period, which was systematically monitored using a high-precision laboratory balance. The slow evaporation of volatile components, primarily monomeric styrene, was indirectly inferred from this continuous mass reduction rather than being directly chemical quantified. After 30 days, the total weight loss was slightly higher for the control samples (~5.5%) compared to the thickened samples (~4.0%).

Table 1
Experimental parameters and corresponding dynamic viscosity evolution of the VE-MgO formulation during the maturation process.

Elapsed Time (days)	Viscosity (cP)	Spring Torque (%)	Rotational Speed (rpm)	Spindle (−)
0	3840	24	100	s91
1	5600	35	100	
2	10450	39.2	60	
3	18690	58.4	50	
4	25170	47.2	60	s92
7	93120	58.2	50	s93
9	143200	53.7	30	
11	202000	50.5	20	
14	232800	58.2	20	
16	336700	50.5	12	
18	424800	53.1	10	
21	431200	53.9	10	
23	439200	54.9	10	
25	461600	57.7	10	
28	460800	57.6	10	
30	480800	60.1	10	

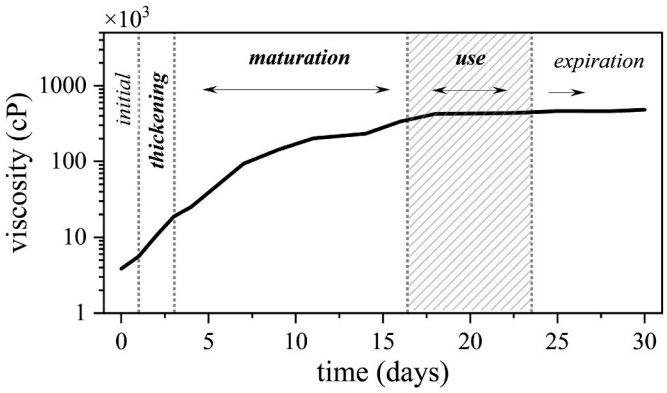

Fig. 2. Evolution of viscosity for the VE-MgO formulation (logarithmic axis) over a 30-day period as measured by Brookfield viscometry. The curve highlights the distinct maturation stages: the initial liquid state (including induction), the rapid thickening phase, maturation, the industrial use window, and final expiration.

Regarding dimensional changes (Fig. 3b), the sample thickness estimated from ultrasonic thickness resonances showed distinct behaviors. The VE-Ref control maintained a constant thickness within the measurement uncertainty. In contrast, the VE-MgO samples displayed a noisy but measurable slight reduction in thickness over time, consistent with the volumetric compaction associated with the maturation process. This contraction has a direct physical impact on the sample volume and, consequently, its density. Rather than assuming a constant density which could introduce systematic errors in the elastic modulus calculation, the density of the resin was calculated at each measurement point by coupling the ultrasonic thickness estimation with the cumulative gravimetric weight loss. Due to the rigid lateral confinement of the aluminum sample containment, the volumetric contraction was dominated by this axial thickness reduction. Because this physical volume contraction significantly outpaced the minor cumulative mass loss from volatile styrene evaporation, the density of the VE-MgO formulation physically increased over time, evolving from an initial value of around 1070 kg/m^3 to approximately 1200 kg/m^3 at Day 21.

4.3. Monitoring of ultrasonic parameters

The evolution of the ultrasonic response was monitored by analyzing the transmission coefficient spectra over the whole thickening process. For the sake of clarity, Fig. 4 displays representative spectra acquired at different aging times. For the VE-Ref control (Fig. 4a), the resonance peaks remained remarkably stable in terms of frequency position (f_n), peak magnitude, and bandwidth throughout the experiment. Only minor frequency shifts towards higher values were observed, primarily attributed to the slight reduction in thickness over time (Fig. 3b) and minor spatial repositioning of the sample holder between measurements. Conversely, the VE-MgO spectra (Fig. 4b) exhibited a progressive and significant evolution: the resonance peaks shifted slightly towards higher frequencies, the peak magnitude decreased dramatically, and the bandwidth broadened (lower Q-factor) as the maturation process progressed.

The longitudinal velocity (v_L) and attenuation (α) calculated from the ultrasonic transmission coefficient spectra measured are presented in Fig. 5. While both parameters remained almost constant for the VE-Ref samples, exhibiting only a minor gradual decrease that is consistent with the slight thickness reduction due to volatile monomer evaporation describe in section 4.2., a pronounced and clear increase in both parameters was observed for the active VE-MgO samples.

Table 2
Definition of the Pre-cure Maturation Stages in SMC resin manufacturing.

Process	Stage	Time[a]	Description
SMC manufacturing	*Initial*	0 – 1 h	The resin is fluid, suitable for fiber impregnation.
	Induction	1 – 12 h	Thickening begins, but the material remains liquid.
	Rapid thickening	1 – 3 days	Viscosity increases rapidly; this is the optimal time for SMC manufacturing.
Composite moulding	*Maturation*	3 – 15 days	Viscosity stabilized; good handling and tackiness for storage.
	Use	16 – 21 days	Non-tacky. This is the optimal time to consolidate the composite.
-	*Expiration*	>21 days	Viscosity is too high; the SMC is expired and cannot be adequately processed.

[a] All time intervals refer to approximate ranges representing the phenomenological stages of the SMC maturation process.

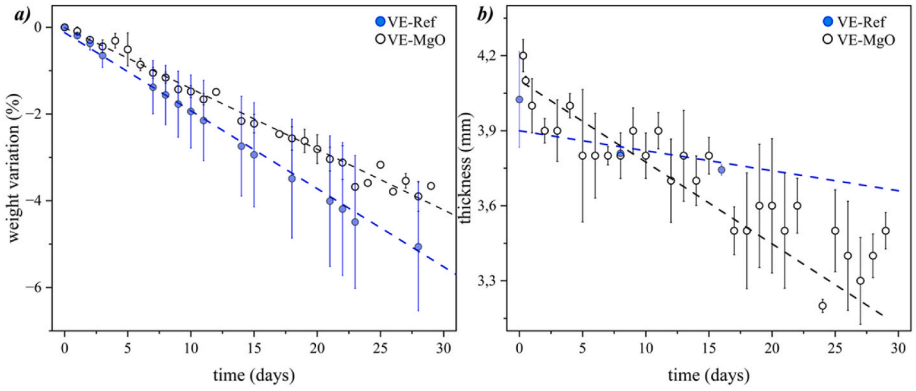

Fig. 3. Physical changes in the resin samples during the 30-day monitoring period. (a) Weight loss percentage for VE-Ref (blue circles) and VE-MgO (empty circles). (b) Thickness changes for VE-Ref (blue circles) and VE-MgO (empty circles). In both plots, symbols represent the mean value, error bars indicate standard deviation, and dashed lines correspond to linear fittings. (N(VE-Ref) = 2; N(VE-MgO) = 5). (For interpretation of the references to colour in this figure legend, the reader is referred to the Web version of this article.)

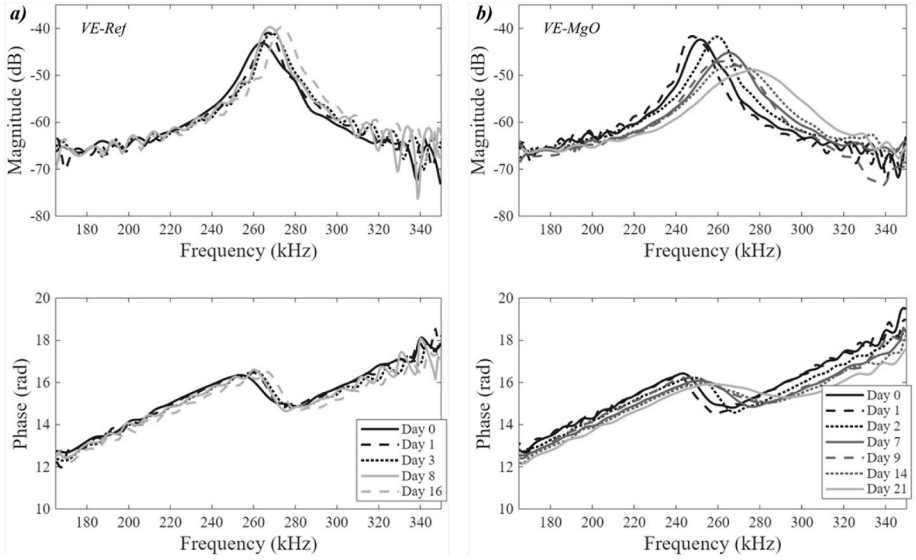

Fig. 4. Representative ultrasonic transmission coefficient spectra (magnitude and phase) acquired at different maturation times indicated in the legends for (a) VE-Ref control and (b) thickened VE-MgO resin.

In the case of v_L (Fig. 5a), for the VE-MgO samples followed a stable, quasi-linear progression rising from 2025 at day 0 to 2075 m/s at day 22. On the other hand, α exhibited a rapid and sharp initial increase, rising from around 10 Np/m at day 0 to 20 Np/m day 20, after which the rate slowed down and gradually stabilized after an increment clear beyond day 22, where also the deviation rises.

4.4. Relationships between ultrasonic and rheological data

To compare the ultrasonic response with the mechanical hardening of the resin, the longitudinal modulus (M) was calculated ($M = \rho \cdot v_L^2$) and is presented in Fig. 6. The control formulation (VE-Ref) maintained a stable modulus of approximately 4.4 GPa throughout the monitoring period. Conversely, the active VE-MgO formulation showed a progressive and monotonic stiffening trend, with M increasing by approximately 50% (from 4.0 GPa to 6.0 GPa) over the 30-day period monitoring window.

Finally, Fig. 7 superimposes the temporal evolution of the derived ultrasonic parameters M and α for the VE-MgO samples onto the distinct maturation stages defined by the Brookfield viscosity curve (previously

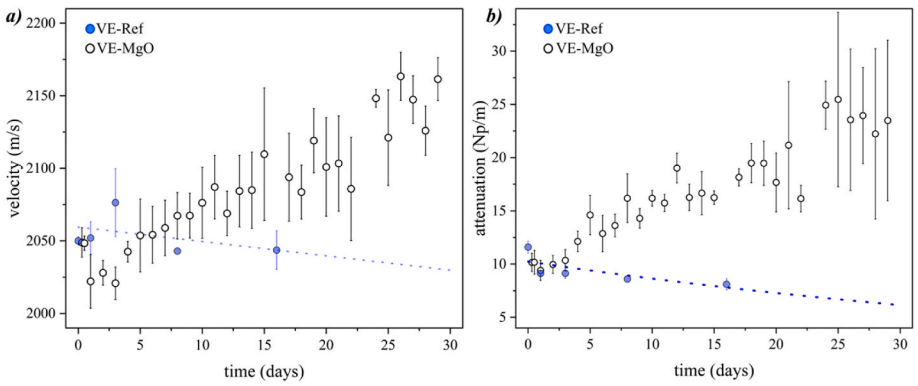

Fig. 5. Ultrasonic parameters trends extracted from transmission coefficient spectra over the 30-day monitoring period. (a) Longitudinal velocity (v_L) and (b) attenuation (α). Blue circles represent the mean values and corresponding standard deviation for VE-Ref samples, with dashed blue lines showing the corresponding linear fittings. Empty circles represent the mean values for VE-MgO samples, where error bars indicate standard deviation (N(VE-Ref) = 3; N(VE-MgO) = 6). (For interpretation of the references to colour in this figure legend, the reader is referred to the Web version of this article.)

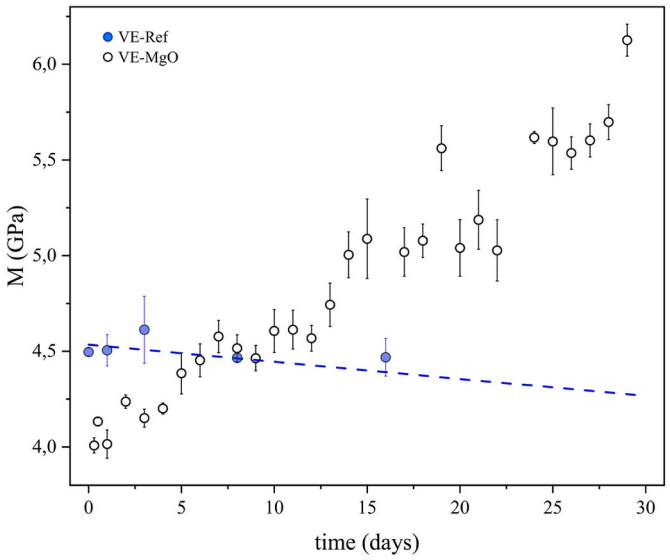

Fig. 6. Calculated longitudinal Modulus (M) versus time for VE-Ref (blue circles represent the mean and error bars the standard deviation; blue dashed line represents the linear fitting) and VE-MgO. Empty circles represent the mean and error bars the standard deviation. (N(VE-Ref) = 3; N(VE-MgO) = 6). (For interpretation of the references to colour in this figure legend, the reader is referred to the Web version of this article.)

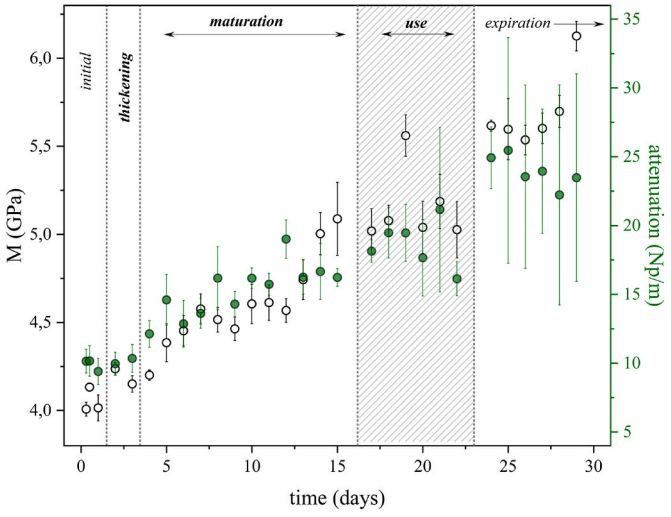

Fig. 7. Longitudinal Modulus (M, empty circles) and attenuation (α, green circles) for the VE-MgO formulation overlaid with the maturation stages defined by apparent viscosity measurements. Circles represent mean, error bars standard deviation. (N(*VE-MgO*) = 6). (For interpretation of the references to colour in this figure legend, the reader is referred to the Web version of this article.)

presented in Fig. 2).

As summarized in Table 3, both *M* and α remained relatively low and stable during the initial *Induction* stage (days 0 to 1). The transition to *Rapid Thickening* stage (approx. day 2-3) coincided with the onset of the increase in both ultrasonic parameters. Throughout the *Maturation* and *Use* stages (days 4 to 23), a continuous, gradual and stable progression in both parameters towards a plateau was observed, suggesting the steady growth of the early physical ionic network. Upon entering the *Expiration* zone (beyond day 23), the data points for both modulus and attenuation exhibited a deviation from the previous smooth maturation trends. This final stage is marked by a noticeable increase in both the measurement means and the dispersion, which is likely associated with the appearance of heterogeneities or potential micro-voids that induce scattering rather than viscoelastic absorption. The apparent viscosity ranges in Table 3 are reported as approximate intervals, since the maturation-stage boundaries are phenomenological and the experimental uncertainty does not justify a higher numerical precision.

Table 3
Value ranges of days, viscosity, attenuation and elastic modulus at each SMC stage.

Stage	Days	Viscosity (cP)	Attenuation (Np/m)	Elastic Modulus (GPa)
Initial/ Induction	0 – 1	$4.0 \times 10^3 - 6.0 \times 10^3$	9.4 – 10.2	4.0 – 4.1
Rapid thickening	2 – 3	$1.0 \times 10^4 - 2.0 \times 10^4$	9.9 – 10.4	4.1 – 4.2
Maturation	4 - 16	$2.5 \times 10^4 - 3.4 \times 10^5$	12.1 – 19.0	4.2 – 5.1
Use	17 - 23	$4.2 \times 10^5 - 4.4 \times 10^5$	16.1 – 21.2	5.1 – 5.6
Expiration	>23	$>4.5 \times 10^5$	>21	>5.6

5. Discussion

The aim of this study was to evaluate whether longitudinal ultrasonic wave parameters could serve as effective proxies for monitoring the viscosity-driven thickening of vinyl ester resins, a process traditionally

characterized by shear properties. The justification for this approach lies in the practical limitation of shear wave propagation in liquid and semi-solid media, which is particularly challenging for air-coupled techniques due to the high acoustic impedance mismatch. While the bulk modulus (K) dominates the longitudinal modulus ($M = K + 4/3\ G$) in the early, low-viscosity stages, we hypothesized that the early formation of the ionic network, which drives the thickening, would induce a measurable increase in the shear modulus (G) and, crucially, impose significant restrictions on polymer chain mobility.

Our results partially confirm this hypothesis, revealing that the sensitivity of the parameters is highly dependent on the stage of the maturation process. During the initial induction phase (typically the first 3 days), the longitudinal velocity (v_L) shows limited sensitivity. In this highly fluid regime, the mechanical response is heavily dominated by the K, associated with volume compressibility, which remains relatively constant, while the contribution of the G is masked. Conversely, the ultrasonic attenuation (α) emerges as a more sensitive indicator during these early stages. This behavior can be explained by the viscoelastic nature of the resin, where attenuation is highly sensitive to energy dissipation arising from molecular friction. As the thickening agent begins to interact with the polymer, it initiates the formation of localized clusters. While these microstructural changes are not yet sufficiently developed to build measurable macroscopic stiffness, they can impose immediate restrictions on the mobility of the polymer chains. This restriction increases the internal viscoelastic friction and can be attributable to the high-frequency energy dissipation that our results suggest, before major changes occur in velocity. However, other reasons such as increased scattering due to micro-heterogeneities can increase the attenuation specially at the final stages.

The comparative analysis with the control formulation (VE-Ref) establishes a critical baseline. The remarkable stability of the neat resin in terms of velocity, attenuation, and estimated modulus (Figs. 5 and 6) effectively minimizes the likelihood of environmental factors or volatile evaporation acting as the primary drivers of the observed ultrasonic changes. This distinct behavior strongly suggests that the physical evolution observed in the VE-MgO samples is primarily associated with the chemorheological interactions induced by the thickening agent. Consequently, under the conditions studied, these ultrasonic parameters can be considered reliable indicator of the resin's physical maturation.

Furthermore, the correlation with standard rheological data strengthens this validation when analyzing the complete thickening process until expiration. As illustrated in the combined analysis (Fig. 7), the ultrasonic trends qualitatively mirror the phenomenological maturation stages defined by the Brookfield viscometer, although the technique allows to identify the transition between key industrial windows. The initial induction phase corresponds to a relatively flat ultrasonic response, reflecting the physical limitations of the setup in detecting the very early molecular associations. However, the onset of rapid thickening is marked by a clear inflection point where both M and attenuation rise significantly, signaling the entry into the “Use window” where tack and handleability are optimal. Crucially, as the material reaches the “Expiration zone”, the trends deviate from early rapid growth as well as the dispersion increases. This transition is highly valuable for industrial staging: while conventional control relies on operator-dependent qualitative assessments, the NC-RUS technique provides a contactless marker of the thickening stages of the resin, particularly use and expiration windows.

This methodology offers a distinct advantage over conventional polymer testing: it is non-contact and non-destructive. This allows for in-situ, real-time characterization, particularly valuable during the “use window” of SMC, where maintaining tack and handleability is critical. Unlike probe-based methods, ACU verifies this state without risk of contamination or mechanical disruption of the evolving matrix.

5.1. Limitations and future work

Nonetheless, certain limitations in the current work must be addressed to guide future developments. First, the experimental monitoring was conducted under typical laboratory conditions with temperature variations of ±2 °C and relatively small sample size in terms of the first thickening stages. While current results show the potential of this technique even under thermal fluctuations not far from real-world industrial environments, further systematic testing is required to strengthen statistical validation. Additionally, although the use of longitudinal wave parameters to infer a shear-dominated network evolution is physically supported by previous referenced works and the presented experimental results, the individual contributions of the bulk (K) and shear (G) moduli to the overall longitudinal modulus (M) have not been quantitatively decoupled in this study.

Second, during the “expiration zone” (beyond day 20), the observed attenuation and signal dispersion may not be solely due to pure viscoelastic absorption. At these high thickening levels, the formation of heterogeneous clusters and potential micro-voids within the semi-solid matrix can introduce acoustic scattering.

To overcome these limitations and address the aspect not fully covered in this study, future work will focus on: (i) increasing the sample size (N) to perform a deeper statistical validation; (ii) investigating the influence of acoustic scattering in highly thickened media including glass fibers as typically SMC contains; and (iii) developing advanced model to quantitatively decoupled the temporal evolution of K and G moduli contributions from the longitudinal wave parameters.

6. Conclusions

This study validates Non-Contact Resonant Ultrasound Spectroscopy (NC-RUS) as a reliable in-situ tool for monitoring the pre-cure maturation phase of vinyl ester resins. We confirmed that the ionic thickening process can be tracked by the combined analysis of parameters directly obtained from the ultrasonic response such as longitudinal attenuation and the elastic modulus, demonstrating the method's sensitivity to the viscoelastic damping associated with the early formation bonds of the polymer network. Remarkably, a clear correspondence was identified between the ultrasonic changes in time due to maturation and the established rheological stages defined by Brookfield viscometry, thereby confirming the ultrasonic parameters as indicators of the underlying chemorheological transformation.

The proposed methodology based on Air-Coupled Ultrasound (ACU) offers a significant practical advantage over current destructive techniques by enabling non-contact, real-time verification of the resin state, facilitating a pivotal shift from reactive quality control to active process monitoring. However, establishing a precise quantitative calibration remains challenging due to the reliance of current industrial criteria on empirical, batch-dependent viscosity ranges rather than standardized, objective thresholds. Future work must focus on addressing the complexity introduced by fiber-reinforced Sheet Moulding Compound (SMC) sheets and developing robust phenomenological models to translate these results into quantitative ranges adaptable to control limits for industrial deployment.

CRediT authorship contribution statement

Lola Fariñas: Funding acquisition, Investigation, Methodology, Validation, Visualization, Writing – original draft. **Beatriz Achiaga:** Writing – review & editing. **Marta Camacho-Iglesias:** Conceptualization, Investigation, Writing – review & editing. **Rafael García-Etxabe:** Funding acquisition, Project administration, Resources, Supervision, Writing – review & editing.

Declaration of competing interest

The authors declare the following financial interests/personal relationships which may be considered as potential competing interests: Lola Farinas reports financial support was provided by Basque Government. Lola Farinas reports financial support was provided by Spain Ministry of Science Innovation and Universities. If there are other authors, they declare that they have no known competing financial interests or personal relationships that could have appeared to influence the work reported in this paper.

Acknowledgements

This work was supported by the Government of the Basque Country through Elkartek Program under Grant KK-2024/00037 (MOSINCO). L. Fariñas acknowledges financial support in part by MICINN (Spain) through the program Juan de la Cierva-Inc. under Grant JC2020-043487-I, and in part by the European Union NextGenerationEU.

Data availability

Data will be made available on request.

References

[1] Mazumdar S. Composites manufacturing: materials, product, and process engineering. 0 ed. CRC Press; 2001. https://doi.org/10.1201/9781420041989.
[2] Li H. Synthesis, characterization and properties of vinyl ester matrix resins. Virginia Tech; 1998. http://vtechworks.lib.vt.edu/handle/10919/30521.
[3] Aragão RDA, Azevedo IT, Soares K. Process-property relationships of sheet molding compound composites with calcium carbonate and hollow-glass microsphere loadings. Mater Sci Technol 2025:02670836251340121. https://doi.org/10.1177/02670836251340121.
[4] Han CD, Lem K. Chemorheology of thermosetting resins. I. The chemorheology and curing kinetics of unsaturated polyester resin. J Appl Polym Sci 1983;28:3155–83. https://doi.org/10.1002/app.1983.070281014.
[5] Lunetto V, Galati M, Settineri L, Iuliano L. Sustainability in the manufacturing of composite materials: a literature review and directions for future research. J Manuf Process 2023;85:858–74. https://doi.org/10.1016/j.jmapro.2022.12.020.
[6] Gandhi KS, Burns R. Studies on the thickening reaction of polyester resins employed in sheet molding compounds. J Polym Sci Polym Chem Ed 1976;14:793–811. https://doi.org/10.1002/pol.1976.170140402.
[7] Wailem Kwok, Han CD. Rheology of unsaturated polyester resins. III. Effects of filler and low-profile additive on the thickening behavior of unsaturated polyester resin. J Appl Polym Sci 1983;28:779–93. https://doi.org/10.1002/app.1983.070280230.
[8] Hall M, Zeng X, Shelley T, Schubel P. In situ thermoset cure sensing: a review of correlation methods. Polymers 2022;14:2978. https://doi.org/10.3390/polym14152978.
[9] Polychronopoulos ND, Vlachopoulos J. Polymer processing and rheology. In: Jafar Mazumder MA, Sheardown H, Al-Ahmed A, editors. Functional polymers. Cham: Springer International Publishing; 2019. p. 133–80. https://doi.org/10.1007/978-3-319-95987-0_4.
[10] Müller-Pabel M, Rodríguez Agudo JA, Gude M. Measuring and understanding cure-dependent viscoelastic properties of epoxy resin: a review. Polym Test 2022;114:107701. https://doi.org/10.1016/j.polymertesting.2022.107701.
[11] Papadakis EP. Monitoring the moduli of polymers with ultrasound. J Appl Phys 1974;45:1218–22. https://doi.org/10.1063/1.1663392.
[12] Lindrose AM. Ultrasonic wave and moduli changes in a curing epoxy resin: ultrasonic techniques are examined as a means for monitoring reaction extent and the development of solid-phase moduli in a curing epoxy. Exp Mech 1978;18:227–32. https://doi.org/10.1007/BF02328418.
[13] Mason WarrenP, McSkimin HJ. Mechanical properties of polymers at ultrasonic frequencies. Bell Syst Tech J 1952;31:122–71. https://doi.org/10.1002/j.1538-7305.1952.tb01379.x.
[14] Baker WO, Mason WP, Heiss JH. Mechanical properties of discrete polymer molecules. J Polym Sci 1952;8:129–55. https://doi.org/10.1002/pol.1952.120080201.
[15] Rokhlin SI, Lewis DK, Graff KF, Adler L. Real-time study of frequency dependence of attenuation and velocity of ultrasonic waves during the curing reaction of epoxy resin. J Acoust Soc Am 1986;79:1786–93. https://doi.org/10.1121/1.393240.
[16] Freemantle RJ, Challis RE. Combined compression and shear wave ultrasonic measurements on curing adhesive. Meas Sci Technol 1998;9:1291–302. https://doi.org/10.1088/0957-0233/9/8/023.
[17] Challis RE, Unwin ME, Chadwick DL, Freemantle RJ, Partridge IK, Dare DJ, Karkanas PI. Following network formation in an epoxy/amine system by ultrasound, dielectric, and nuclear magnetic resonance measurements: a comparative study. J Appl Polym Sci 2003;88:1665–75. https://doi.org/10.1002/app.11822.
[18] Ghodhbani N, Maréchal P, Duflo H. Ultrasound monitoring of the cure kinetics of an epoxy resin: identification, frequency and temperature dependence. Polym Test 2016;56:156–66. https://doi.org/10.1016/j.polymertesting.2016.10.009.
[19] Lionetto F, Maffezzoli A. Polymer characterization by ultrasonic wave propagation. Adv Polym Technol 2008;27:63–73. https://doi.org/10.1002/adv.20124.
[20] Lionetto F, Maffezzoli A. Monitoring the cure state of thermosetting resins by ultrasound. Materials 2013;6:3783–804. https://doi.org/10.3390/ma6093783.
[21] Houhat N, Devaux T, Callé S, Saengdee L, Boucaud Gauchet S, Vander Meulen F. Monitoring of polymer viscosity by simultaneous ultrasonic and rheological measurements at high and varying temperatures. AIP Adv 2025;15:035235. https://doi.org/10.1063/5.0251850.
[22] Maia NA, Pereira FR, Cella N. Pulse-echo ultrasonic measurements of compressibility coefficient of thick epoxy resin during the curing process. Mater Today Commun 2018;17:194–9. https://doi.org/10.1016/j.mtcomm.2018.09.007.
[23] Lakes RS. Viscoelastic measurement techniques. Rev Sci Instrum 2004;75:797–810. https://doi.org/10.1063/1.1651639.
[24] Wang Y, Challis RE, Phang AP-Y, Unwin ME. Bulk shear wave propagation in an epoxy: attenuation and phase velocity over five decades of frequency. IEEE Trans Ultrason Ferroelectrics Freq Control 2009;56:2504–13. https://doi.org/10.1109/TUFFC.2009.1337.
[25] Truell R, Elbaum C, Chick BB. Ultrasonic methods in solid state physics. Academic Press, Inc.; 1969.
[26] Saggin R, Coupland JN. Oil viscosity measurement by ultrasonic reflectance. JAOCS J Am Oil Chem Soc 2001;78:509–11. https://doi.org/10.1007/s11746-001-0294-z.
[27] Simonetti F, Cawley P. A guided wave technique for the characterization of highly attenuative viscoelastic materials. J Acoust Soc Am 2003;114:158–65. https://doi.org/10.1121/1.1575749.
[28] Dixon S, Jaques D, Palmer SB. The development of shear and compression elastic moduli in curing epoxy adhesives measured using non-contact ultrasonic transducers. J Phys D Appl Phys 2003;36:753–9. https://doi.org/10.1088/0022-3727/36/6/319.
[29] Lionetto F, Tarzia A, Coluccia M, Maffezzoli A. Air-coupled ultrasonic cure monitoring of unsaturated polyester resins. Macromol Symp 2007;247:50–8. https://doi.org/10.1002/masy.200750107.
[30] Dominguez-Macaya A, Álvarez-Arenas TEG, Saenz-Dominguez I, Tena I, Aurrekoetxea J, Iturrospe A. Monitoring the evolution of stiffness during ultraviolet curing of a vinyl ester resin with quasi-normal air-coupled ultrasonic spectroscopy. Polym Test 2019;80:106112. https://doi.org/10.1016/j.polymertesting.2019.106112.
[31] Han CD, Lem K. Rheology of unsaturated polyester resins. II. Thickening behavior of unsaturated polyester and vinyl ester resins. J Appl Polym Sci 1983;28:763–78. https://doi.org/10.1002/app.1983.070280229.
[32] Liu W, Jiao W, Yang F, Wang R, Li L, Jiao W. Study on rheological behavior of vinyl ester resin during thickening. Vinyl Addit Technol 2018;24:239–47. https://doi.org/10.1002/vnl.21572.
[33] Kinra VK, Iyer VR. Ultrasonic measurement of the thickness, phase velocity, density or attenuation of a thin-viscoelastic plate. Part I: the forward problem. Ultrasonics 1995;33:95–109. https://doi.org/10.1016/0041-624X(94)00025-K.
[34] Kinra VK, Iyer VR. Ultrasonic measurement of the thickness, phase velocity, density or attenuation of a thin-viscoelastic plate. Part II: the inverse problem. Ultrasonics 1995;33:111–22. https://doi.org/10.1016/0041-624X(94)00026-L.
[35] Gómez Álvarez-Arenas TE. Simultaneous determination of the ultrasound velocity and the thickness of solid plates from the analysis of thickness resonances using air-coupled ultrasound. Ultrasonics 2010;50:104–9. https://doi.org/10.1016/j.ultras.2009.09.009.
[36] Álvarez-Arenas TEG, Gil-Pelegrin E, Ealo Cuello J, Fariñas M, Sancho-Knapik D, Collazos Burbano D, Peguero-Pina J. Ultrasonic sensing of plant water needs for agriculture. Sensors 2016;16:1089. https://doi.org/10.3390/s16071089.
[37] Türk O, Vargiolu G, Dippon K, Busam N, Weber S. Sheet molding compounds (smc), thick molding compounds (tmc), and bulk molding compounds (bmc) comprising thermosetting resins based on renewable resources, PCT/EP2007/006659. https://patents.google.com/patent/EP2046859B1/en; 2009.